Biochimica et Biophysica Acta 1813 (2011) 412–423

Contents lists available at ScienceDirect

Biochimica et Biophysica Acta

journal homepage: www.elsevier.com/locate/bbamcr

TRP expression pattern and the functional importance of TRPC3 in primary human T-cells

Anna S. Wenning [1], Katherina Neblung [1], Bettina Strauß, Melodie-Jo Wolfs, Anne Sappok, Markus Hoth, Eva C. Schwarz *

Department of Biophysics, Gebäude 58, University of the Saarland, D-66421 Homburg/Saar, Germany

ARTICLE INFO

Article history:
Received 19 January 2010
Received in revised form 22 December 2010
Accepted 23 December 2010
Available online 4 January 2011

Keywords:
TRP channel
Primary human T-cell
Calcium
Jurkat T-cell
Quantitative RT-PCR
siRNA

ABSTRACT

TRP proteins form ion channels which are activated following receptor stimulation. In T-cell lines, expression data of TRP proteins have been published. However, almost no data about TRP expression is available in primary human T-cells. Using RT-PCR and quantitative RT-PCR, we compare the expression of TRP mRNA in 1) human peripheral blood lymphocytes, which are a mix of mostly mono-nuclear blood lymphocytes but contain other leucocytes, 2) a pure human $CD4^+$ T-helper cell population in the resting (=naïve) and activated (=effector) state, and 3) two commonly used $CD4^+$ Jurkat T-cell lines, E6-1 and parental. To mimic physiological cell stimulation, we analyzed TRP expression in primary human cells in a quantitative way over several days following formation of an immunological synapse through stimulation with antibody-coated beads. The TRP expression profile of primary human T-cells was significantly different from Jurkat T-cells. Among the TRP mRNAs of the TRPC, TRPM, and TRPV family, we found consistent expression of TRPC1, TRPC3, TRPV1, TRPM2, and TRPM7 in primary human $CD4^+$ T-cells of all analyzed blood donors. Among these, TRPC3 and TRPM2 were strongly up-regulated following stimulation, but with different kinetics. We found that TRPC3 modulates Ca^{2+}-dependent proliferation of primary $CD4^+$ T-cells indicating that TRPC3 may be involved in Ca^{2+} homeostasis in T-cells besides the well-established STIM and ORAI proteins which are responsible for store-operated Ca^{2+} entry.

1. Introduction

The activation of $CD4^+$ T-cells is central to the adaptive immune response. T-cells are activated by foreign antigens which are transported to the T-cell zones in lymph nodes by antigen-presenting cells (APC). Antigens are then presented by the APC through class-II major histocompatibility (MHC) complexes until they encounter the corresponding naïve antigen-specific $CD4^+$ T-cells [1,2]. Antigen recognition through the T-cell receptor (TCR) induces many signaling cascades and molecular re-arrangements within T-cells, which together control the immune response. Subsequent Ca^{2+} influx through Ca^{2+} release-activated Ca^{2+} (CRAC) channels leads to the rise of intracellular Ca^{2+} levels with short-term and long-term consequences for T-cell activation [3]. The formation of the so-called immunological synapse (IS) is a short-term consequence whereas the expression of interleukin-2 (Il-2) and other cytokines, an extensive clonal expansion and differentiation are long-term consequences [3–6].

For a long time, the molecular identity of the Ca^{2+} channel responsible for store-operated Ca^{2+} entry (SOCE) was a mystery since its first electrophysiological characterization in mast cells [7]. In 2005 and 2006, the two key molecules of SOCE have been identified by several independent RNA interference (RNAi) screens, STIM1 [8,9] and ORAI1 [10–12]. There is no doubt that ORAI channels make up store-operated CRAC channels and STIM1 acts as the Ca^{2+} sensor. After the depletion of Ca^{2+} from the endoplasmic reticulum, STIM1 oligomerizes and translocates to discrete puncta at endoplasmic reticulum–plasma membrane junctions, thus activating ORAI1, the pore-forming subunit of the CRAC channel [13–15].

Over a decade, members of the TRP (transient receptor potential) family were considered as good candidates for the molecular basis of store-operated Ca^{2+} entry in many different cell types. Considering the prominent role of ORAI channels, it appears very unlikely that TRPs play any direct role in SOCE in T-cells [16]. Many reports point into the direction that CRAC mediated Ca^{2+} entry is the only Ca^{2+}-influx pathway following TCR activation [17–19]. However, evidence is emerging that other Ca^{2+} entry mechanisms may exist in T-cells [20,21]. In addition a potential role of the TRPC subfamily in SOCE is still controversial [16,22–28].

Abbreviations: APC, antigen-presenting cells; $[Ca^{2+}]_i$, intracellular Ca^{2+} concentration; CRAC channel, Ca^{2+} release-activated Ca^{2+} channel; IL-2, interleukin-2; IS, immunological synapse; o/n, over night; NCX, Na^+/Ca^{2+} exchanger; PBLs, peripheral blood lymphocytes; RNAi, RNA interference; RT, room temperature; S.D., standard deviation; SEM, standard error of the mean; SOCE, store-operated Ca^{2+} entry; TCR, T-cell receptor; TRP, transient receptor potential

* Corresponding author. Tel.: +49 6841 1626458; fax: +49 6841 1626060.
E-mail address: eva.schwarz@uks.eu (E.C. Schwarz).

[1] These authors contributed equally to the manuscript.

0167-4889/$ – see front matter © 2011 Elsevier B.V. All rights reserved.
doi:10.1016/j.bbamcr.2010.12.022

In humans, the TRP family consist of 6 subfamilies, TRPC, TRPV, TRPM, TRPA, TRPP and TRPML. They form cation-conducting ion channels which share 6 transmembrane domains (for review see [29]). The TRPC subfamily are non-selective ion-channels conducting Na^+, K^+ and Ca^{2+} ions. There is a controversial wealth of literature describing activation and regulation mechanisms of different TRPC proteins and their contribution to SOCE activity which might at least be partially explained by using varying over-expressing systems implicating varying expression levels (summarized in [16]). A general agreement exists about store-independent activation of the TRPC3/6/7 subfamily which is gated by diacylglycerol (DAG), a product of phospholipase C (PLC) hydrolysis of phosphatidylinositol-4,5-bisphosphate [30].

Much less is known about members of the TRPC subfamily in native tissues and their physiological functions. In mice lacking *Trpc1*, thapsigargin, carbacholamin and IP_3-stimulated SOCE in submandibular glands acinar cells was reduced resulting in impaired salivary gland fluid secretion [31]. In TRPC3 knock-out mice, it was shown that TRPC3 functions as a store-operated channel mediating Ca^{2+} influx in acinar cells and the deletion of *Trpc3* led to reduced frequency of Ca^{2+} oscillations [32]. Recently, Riccio et al. [33] published that TRPC5 knock-out mice show less fear in response to aversive stimuli than the wild-type mice. Expression of TRPC1 and TRPC3-C7 was found in vascular smooth muscle tissue of human, rat and rabbit where they contribute to receptor-activated channels (TRPC3, TRPC6, TRPC7), directly stimulated by DAG, or store-operated channels (TRPC1, TRPC5, TRPC6, TRPC7) forming channels of homo- or heterotetrameric subunit compositions [34]). In rat ventricular cardiomyocytes, TRPC3 was also found to be closely associated with the Na^+/Ca^{2+} exchanger (NCX) within the plasma membrane was and it is triggered by PLC suggesting a mechanism to control cardiac Ca^{2+} homeostasis [35–37].

In the present study, we have investigated TRP expression of the three closely related subfamilies TRPC, TRPV and TRPM. We compared expression in primary peripheral blood lymphocytes, $CD3^+$ T-cells and Jurkat T-cell lines. To analyze a potential role of TRPs in development from naïve to effector T-cells, we stimulated $CD4^+$ T-cells with anti-CD3/anti-CD28 coated beads and analyzed the regulation of expression by quantitative RT-PCR after formation of an immunological synapse. We found that TRPC3 was highly up-regulated during stimulation and that down-regulation of TRPC3 with siRNA reduced not only proliferation of $CD4^+$ T-cells but also resting Ca^{2+} in naïve $CD4^+$ T-cells.

2. Materials and methods

2.1. Cells and medium

PBLs were purified as described previously [38]. $CD4^+$ T-cells were negatively isolated using the $CD4^+$ Negative Isolation Kit (Invitrogen, #113.17D) following the manufacturer's instruction. For $CD3^+$ T-cell isolation by FACS, PBLs were stained with anti-CD3/FITC conjugated antibody (Dako, #F0818), washed, and 5×10^7 PBLs were resuspended in 2.25 ml PBS/2.5% BSA. $CD3^+$ T-cells were sorted to the highest purity using the single cell mode of a MoFlo cell sorter (Dako). Following isolation, the purity of $CD4^+$ or $CD3^+$ populations was analyzed by fluorescence microscopy with anti-CD4/RPE or anti-CD3/conjugated antibodies. PBLs were stained with anti-CD4/RPE, anti-CD8/RPE-Cy5 and anti-CD19/FITC and $CD3^+$ T-cells with anti-CD3/FITC conjugated antibodies (Dako, #R0805, #C7079, #F0768, #F0818). PBLs and $CD4^+$ T-cells were cultured in AIMV medium (Invitrogen, #12055-091) supplemented with 10% FCS. The two Jurkat T-cell lines, the so called parental Jurkat T-cell line (par, diphtheria toxin-resistant version of Jurkat T-cells generated by Fanger et al. [39] and E6-1 (#TIB-152, ATCC) were grown in RPMI-1640 (Invitrogen #21875-034) and stably expressing TRPC3 HEK-293 cells in D-MEM medium (including 250 μg/ml G418, Invitrogen #10131-019) supplemented with 10% FCS, 100 U/ml penicillin and 100 μg/ml streptomycin (PAA, #P11-010). Cells were kept at 37 °C (5% CO_2, 95% humidity) and diluted every 2 to 3 days (Jurkat T-cells) or every 3 to 5 days (HEK-293 cells).

2.2. Reagents

All chemicals not specifically mentioned were from Sigma (highest grade).

2.3. Molecular biology

Isolation of total RNA was carried out using the TRIzol® Reagent (Invitrogen, #15596018) including 1 μl Glycogen (5 μg/μl, Invitrogen, #10814-010) according to the manufacturer's protocol. Templates made from total RNA for conventional RT-PCR were prepared from 6.1×10^6 to 1.0×10^8 cells and 1.0–5.3 μg total RNA were reverse transcribed into cDNA by SuperScript™ II reverse transcriptase (Invitrogen, #18064-014) including 1 μl RNaseOut, (Invitrogen, #10777-019) and 1 μl oligo dT Primer (0.5 μg/μl, Invitrogen, #18418-012) following the manufacturer's instruction. mRNA was isolated from $1.2–1.7\times10^8$ PBLs using FastTrack®2.0 mRNA isolation kit (Invitrogen, #K1593-02) and 5 μl were used for reverse transcription. Non-focal stimulation of 1×10^8 PBLs with 2 μg/ml PHA (Sigma, #L9132) and 25 U/ml hIL-2 (Roche, #1204700) for almost 6 days was used as one method to produce an effector cell population. Total RNA from human brain (2 μg/reverse transcription, BD, #640981), kidney (2 μg/reverse transcription, BD, #636529), colon (3.3 μg/reverse transcription), placenta (2.4 μg/RT) and from mouse eye (1.5 μg/reverse transcription) was reverse transcribed as described above. Conventional RT-PCR was carried out in a personal Thermocycler (Biometra) using *Taq*Polymerase from Qiagen (#201203) following standard protocols (20 μl reaction volume, 200 μM dNTPs (Invitrogen, #18427-013), 1 μM each primer, 1.5 mM $MgCl_2$, 0.5 μl cDNA and 0.5 U *Taq*Polymerase). Initial denaturation time was 3 min at 94 °C, followed by 35 cycles with 45 s denaturation (94 °C), 30 s annealing (56–60 °C, depending on each primer pair, for TRPC4 and TRPC5 annealing was 45 s) and 30 s elongation (72°, for TRPM6 and TRPM8 elongation was prolonged to 45 s), and a final extension of 10 min (72 °C). If necessary, 1× Q-solution (Qiagen, #201203) was added to increase specificity. A 10 μl of each PCR reaction was separated on standard agarose gel electrophoresis, images were digitized with a gel documentation system from Herolab. As a marker, the 1-kb Plus DNA ladder from Invitrogen (#10787-018) was used. PCR fragments were cloned using pGEM-T-Vector System I (Promega, #A3600) and confirmed by sequencing (MWG Biotech).

For quantitative RealTime-PCR (qRT-PCR), total RNA was isolated from 8.0×10^6 anti-CD3/anti-CD28 bead stimulated $CD4^+$ T-cells from day 0 (=unstimulated/naïve $CD4^+$ T-cells) to day 13 (on day 1 6.0×10^6 $CD4^+$ T-cells were used). In order to normalize for cell number, 1.5 μl isolated total RNA was used for reverse transcription. QRT-PCR was carried out in a MX3000 instrument from Stratagene. cDNA (0.5 μl) and 300 nM of each primer were set into PCR reactions (25 μl) using Quanti Tect SYBR green kit (Qiagen, #204145) following the manufacturer's instruction. PCR conditions were: initial denaturation, 15 min, 94 °C; 45 cycles: denaturation, 30 s, 94 °C; annealing, 45 s, 58 °C; elongation, 30 s, 72 °C and finally a dissociation curve cycle (60 s, 95 °C; 30 s 55 °C; 30 s 95 °C). Primers were designed using Primer3 program [40] available at WWW (http://frodo.wi.mit.edu/). We tested at least three different primer pairs for each gene. PCR products were analyzed on an agarose gel to detect primer dimers or other unspecific bands. The primer pair with lowest CT value and without any additional band was selected for quantitative PCR. In addition, we performed a melting curve experiment of each PCR reaction, to exclude that different products contaminated the reactions. Expression of genes of interest was normalized to the

expression of the house-keeping genes RNA Polymerase II (#NM_000937) and TATA box-binding protein (#NM_003194).

2.4. Anti-CD25 antibody and F-actin cytoskeleton staining

$CD4^+$ T-cells were settled on poly-L-ornithine-coated (0.1 mg/ml in H_2O, Sigma) glass coverslips for 45–60 min. Cells were washed twice with 1× PBS (pH 7.4), fixed in 3.0% Paraformaldehyde solution for 20 min, incubated in 1× PBS/0.1 M Glycin for 3 min and washed once with 1× PBS. To stain for the F-actin cytoskeleton, $CD4^+$ T-cells were permeabilized with 1× PBS/0.1% Triton. Cells were blocked for 20 min in 1× PBS/2% BSA or 1× PBS/2% BSA/0.1% Triton (following permeabilization) and incubated for 60 min with anti-CD25/PE (1:10, Immunotools, #21330254) or stained with Texas Red®-X phalloidin (1:10, Molecular Probes, #T7471) for 30 min at RT. Cells were washed thrice with 1× PBS (or 1× PBS/0.1% Triton), rinsed in H_2O and embedded in ProLong antifade reagent (Molecular Probes, #P7481) on glass slides. $CD4^+$ T-cells were analyzed on the stage of an Olympus IX 70 microscope equipped with a 20× (UApo/340, N.A. 0.75) or 60× (Uplan FI, N.A. 1.25–0.65, ∞/0.17, oil) objective and filter sets from AHF (HQ-Cy3, #F41-007). Acquisition software was T.I.L.L. Vision.

2.5. Bead stimulation and proliferation experiments

Stimulation with anti-CD3/anti-CD28 coated beads was performed as described before [38]. Shortly, polystyrene microparticles (∅ = 6 μm, Polysciences, #07312) were coated with azide free anti-CD3 mAb (Serotec, #MCA463XZ) and anti-CD28 (BD Pharmingen, #555725) antibodies in a ratio of 1:4 following the manufacturer's protocol. For Ca^{2+} imaging experiments Dynabeads® CD3/CD28 were used (Invitrogen #111-31D). For proliferation experiments in 96 well plates, $CD4^+$ T-cells were stimulated with anti-CD3/anti-CD28 coated beads (ratio cell/bead 1:1) and experiments were carried out as described previously [38]. Proliferation experiments were done under Ca^{2+} limiting conditions by the addition of 1.1 mM EGTA [38]. The number of living cells was determined with CellTiter-Blue™ (Promega, #G8081) following the manufacturer's instruction. Briefly, 20 μl CellTiter-Blue™ was added to each well, plates were shortly shaken and incubated for additional 3 h. Cells were resuspended and fluorescence was measured with a GeniosPro universal microplate reader (Tecan) with an excitation of 535 nm and an emission of 590 nm. Instrument settings were: bottom reading, 30 s normal shaking, 30 s shake settle time, 10 flashes, 40 μs integration time, gain 38. The results were expressed as percentage of relative fluorescence units (RFU). For day 0, cells were cultured for 1 h at 37 °C, 5% CO_2 and 95% before adding 20 μl CellTiter-Blue™ reagent to each well [38].

2.6. Transfection with siRNAs

$CD4^+$ T-cells were transfected using Nucleofector technology (Lonza) as described by the manufacturer. $CD4^+$ T-cells (5×10^6) were transfected with 60 or 100 pmol (for modified siRNAs) siRNA (20 μM). The following siRNAs were used: TRPC3siRNAs (Qiagen, sense 5′ CGU UGU GCU CAA AUA UGA UdT dT 3′, antisense 5′ AUC AUA UUU GAG CAC AAC G dG dA 3′) and the same sequence modified by introducing 2′ deoxy or 2′ methoxy modifications into the siRNA (TRPC3 siRNAmod (C3-1mod), sense 5′ r(OMeU-OMeC-CGU UGU GCU CAA AUA) d(UGA) d(OMeU-OMeT-OMeT) 3′, antisense 5′ d(A) r (UC AUA UUU GAG CAC AAC G-OMeG-OMeA) 3′), non-silencing (#1022076, Qiagen) and STIM1siRNA (Dharmacon, #L-011785-00-0005). On day 1 following transfection, $CD4^+$ T-cells were washed and resuspended in fresh medium. For single cell Ca^{2+} imaging experiments, $CD4^+$ T-cells were transfected on day 0, washed on day 1, stimulated on day 4 (90 h) and measured 1, 2 or 3 days after stimulation. HEK-293 cells were grown in 6-well plates and cells in each well were transfected with 0.6 μl siRNA (20 μM) using HiPerfect (Qiagen, #301705) as described by the manufacturer.

2.7. Single cell Ca^{2+} imaging

$CD4^+$ T-cells were loaded with 2 μM fura-2/AM (Invitrogen) in complete medium at 37 °C for 20 min, washed with fresh medium, stored at 37° for 10 min, and immediately used. Cells were allowed to settle on poly-L-ornithine-coated (0.1 mg/ml) glass coverslip (1.5–3×10^5 cells per coverslip) chambers on the stage of an Olympus IX 70 microscope equipped with a 20× (UApo/340, N.A. 0.75) objective. Cells were alternately illuminated at 340 and 380 nm with a Polychrome V Monochromator (Agilent Technologies, TILL Photonics) using SP 410 as excitation filter and DCLP 410 as dichroic mirror. The fluorescence emissions at $\lambda>440$ nm (LP 440) were captured with a CCD camera (TILL Imago), digitized, and analyzed using TILL Vision software. Ratio images and infrared images were recorded at intervals of 5 s. A sandwiched self-made chamber was used for all measurements which allowed for a complete solution exchange less than 1 s. To analyze Ca^{2+} influx in STIM1, TRPC3 or control siRNA down-regulated $CD4^+$ T-cells, Ca^{2+} stores were depleted by thapsigargin (Invitrogen, 1 μM in Ca^{2+} free Ringer solution), and Ca^{2+} influx was monitored following the re-addition of 0.25 mM Ca^{2+} Ringer solution. To analyze resting $[Ca^{2+}]_i$ in $CD4^+$ T-cells, complete AIMV was used during the whole experiment. All experiments were carried out at 37 °C.

2.8. Data analysis and statistics

Data were analyzed using TILL Vision (Agilent Technologies, TILL Photonics), Igor Pro (Wavemetrics) and Microsoft Excel (Microsoft). To analyze CT values and primer efficiencies of quantitative real time PCR, unprocessed data from MxPro Software were transferred into a macro written for Igor Pro which was kindly provided by the Department of Molecular Cell Biology, Saarland University (Peter Lipp, Gregor Reither and Achim Heinz). SD or SEM was used as indicated in the figure legends. In case, data points were normally distributed, an unpaired two-sided Student's *t*-test was used. If normal distribution could not be confirmed, a non-parametric test (Mann–Whitney) was performed.

3. Results

3.1. Expression of TRPs in primary human T-cells

Ca^{2+} influx plays a central role during the activation of naïve and effector T-cells. Whereas the role of STIM and ORAI proteins for Ca^{2+} influx is undisputed [8–12], the role of members of the TRP family for Ca^{2+} signaling pathways is very controversial. In addition, very little information is available about the expression pattern of TRPC, TRPV and TRPM subfamilies in primary human T-cells. Due to the limited availability of specific and high-affinity antibodies, it is impossible to obtain a complete expression profile of these channels on protein level. Therefore, we analyzed mRNA levels of TRPs with conventional RT-PCR and quantitative RT-PCR. Primer sequences, accession numbers and PCR conditions for the expression of TRPC1-C7, TRPV1-V6 and TRPM1-M8 at the mRNA level by conventional RT-PCR are summarized in Table 1. To obtain a comprehensive view and coincidentally, to avoid the possibility of donor specific expression of single TRPs, we compared expression levels of TRPs in unstimulated peripheral blood lymphocytes (PBLs) from 8 different donors, in naïve $CD3^+$ T-cells from 5 different donors, in PHA/IL-2 stimulated PBLs (= effector cells) from 4 different donors, and in Jurkat T-cell lines (see Table 2). To quantify the different cell types within the PBL population, we investigated purified PBLs by immunohistochemistry (Fig. 1A). The majority of cells were CD3 positive (about 75%) whereas

Table 1
Primers and PCR-conditions for the RT-PCR screen of TRPC, TRPV and TRPM subfamilies.

Gene	Accession	Primer	Sequence 5′–3′	Ann. T.	Position (from start codon ATG)	Length of the RT-PCR product	Q-solution
TRPC1	NM_003304,	forw	5′ ctatggagaagaactgcagtc 3′	58 °C	1734–1754	400 bp	no
	ID:7220	rev	5′ ggaagtcaagtaacgatgcac 3′	58 °C	2113–2133		no
TRPC3	NM_003305	forw	5′ tgttcaatgcctcagacagg 3′	58 °C	1202–1221	343 bp	yes
	ID: 7222	rev	5′ agtgtcacttcactgaggtc 3′	58 °C	1525–1544		yes
TRPC4	NM_016179	forw	5′ tggaacaatagggaggcgag 3′	58 °C	2067–2086	580 bp	yes
	ID: 7223	rev	5′ tctctcaagtggtcctgcag 3′	58 °C	2627–2646		yes
TRPC5	NM_012471	forw	5′ accagagctatcgatgagcc 3′	60 °C	1630–1649	951 bp	yes
	ID: 7224	rev	5′ actgggttcagacatatgacc 3′	60 °C	2560–2580		yes
TRPC6	NM_004621	forw	5′ cttttgctgaaggcaagagg 3′	58 °C	554–573	457 bp	yes
	ID: 7225	rev	5′ ctgcacagatcaaggagtcc 3′	58 °C	991–1010		yes
TRPC7	NM_020389	forw	5′ ctgcacaatgtctcgcttc 3′	58 °C	1534–1552	655 bp	yes
	ID: 57113	rev	5′ tgaggcacatcttgattctc 3′	58 °C	2168–2188		yes
TRPV1	AY131289	forw	5′ acacacctgatggcaaggac 3′	58 °C	2192–2211	232 bp	yes
	ID: 7442	rev	5′ agactgcctatctcgagcac 3′	58 °C	2402–2421		yes
TRPV2	NM_016113	forw	5′ aagcggaggttggaaactcc 3′	58 °C	1271–1290	455 bp	no
	ID: 51393	rev	5′ cactgactctgtggcattgg 3′	58 °C	1706–1725		no
TRPV3	NM_145068	forw	5′ tgcctgacttcctcatgcac 3′	58 °C	461–480	627 bp	yes
	ID: 162514	rev	5′ gactgaggatgtacttcagg 3′	58 °C	1068–1087		yes
TRPV4	NM_021625	forw	5′ acattgtcaactacctgacgg 3′	58 °C	896–916	543 bp	yes
	ID: 59341	rev	5′ acaggtaggagaccacgttg 3′	58 °C	1419–1438		yes
TRPV5	NM_019841	forw	5′ cagagaacaagactgggacc 3′	58 °C	72–91	471 bp	yes
	ID: 56302	rev	5′ tccatgctcaatgagcagc 3′	58 °C	540–558		yes
TRPV6	NM_018646	forw	5′ caagttgctcaagtatgagg 3′	58 °C	186–205	373 bp	yes
	ID: 55503	rev	5′ tccatgctcaatgagcagc 3′	58 °C	540–558		yes
TRPM1	NM_002420	forw	5′ agtggaggaagaaactgacc 3′	58 °C	1116–1135	264 bp	yes
	ID: 4308	rev	5′ aggctgatgtggtaatcagg 3′	58 °C	1360–1379		yes
TRPM2	NM_003307	forw	5′ gtcaagctcaacgtgcagg 3′	56 °C	1783–1801	471 bp	yes
	ID: 7226	rev	5′ attgtccacggagagctgg 3′	56 °C	2235–2253		yes
TRPM3	AJ505026	forw	5′ gagctcacagcaatgttgg 3′	56 °C	2482–2500	728 bp	yes
	ID: 80036	rev	5′ gtctcattctgtccacagg 3′	56 °C	3191–3209		yes
TRPM4	NM_017636	forw	5′ aggtggagaggattatgacc 3′	60 °C	1049–1068	573 bp/457 bp	yes
	ID: 54795	rev	5′ agagcagatacatgctctcc 3′	60 °C	1602–1621		yes
TRPM5	NM_014555	forw	5′ tgtcacctgcaggatgctg 3′	58 °C	2463–2481	321 bp	yes
	ID: 29850	rev	5′ tcatcaatctcgtccagtgg 3′	58 °C	2764–2783		yes
TRPM6	NM_017662	forw	5′ gttcacttacaccgtgttgg 3′	58 °C	2565–2584	822 bp	yes
	ID: 140803	rev	5′ tcttcttggtcgtgaggag 3′	58 °C	3368–3386		yes
TRPM7	NM_017672	forw	5′ gatgatggtcctgtaagacc 3′	60 °C	3838–3857	685 bp	yes/no
	ID: 54822	rev	5′ tgagtgtcttcggtagatgg 3′	60 °C	4504–4522		yes/no
TRPM8	NM_024080	forw	5′ aacagctgctggtctattcc 3′	58 °C	1922–1941	922 bp	yes
	ID: 79054	rev	5′ aggttgtgctcatccagctc 3′	58 °C	2824–2843		yes

Additional primer pairs for TRPC6.

Gene	Accession	Primer	Sequence 5′–3′	Ann. T.	Position (from start codon ATG)	Length of the RT-PCR product	Q-solution
TRPC6	forw	5′ aggttagctaatcgaggacc 3′	58 °C	232–251	TRPC6_forw_232	yes	
TRPC6	forw	5′ cttttgctgaaggcaagagg 3′	58 °C	554–573	TRPC6_forw_554	yes	
TRPC6	forw	5′ ttcctgtacccttcaatctgg 3′	58 °C	2279–2299	TRPC6_forw_2279	yes	
TRPC6	rev	5′ ctgcacagatcaaggagtcc 3′	58 °C	991–1010	TRPC6_rev_991	yes	
TRPC6	rev	5′ tctggagcgtttcaacatcc 3′	58 °C	1044–1063	TRPC6_rev_1044	yes	
TRPC6	rev	5′ agttcatagcggagacttgag 3′	58 °C	2673–2693	TRPC6_rev_2673	yes	

Gene	Primer pair	Length of the RT-PCR product
TRPC6	forw/rev	232/991	760 bp
TRPC6	forw/rev	232/1044	813 bp
TRPC6	forw/rev	554/991	438 bp
TRPC6	forw/rev	554/1044	491 bp
TRPC6	forw/rev	2279/2673	395 bp

around 14% of cells were CD19 positive cells (B-cells). Among the $CD3^+$ T-cells, 75.7 ± 13.9% were CD4 positive and 26.8 ± 9.5% CD8 positive T-cells. For the analysis of naïve $CD3^+$ T-cells, $CD3^+$ T-cells were sorted by FACS under very stringent conditions generating a 100% pure $CD3^+$ T-cell population (see Fig. 1B, 1271 cells out of 1272 cells were CD3 positive analyzed with immunohistochemistry (99.9%)). To stimulate PBLs, 2 μg/ml PHA and 10–25 U/ml IL-2 were added in to the medium over 6 days. Following stimulation, the percentage of $CD3^+$ T-cells increased from 75% to 87.2% (±1.7%) whereas the percentage of $CD19^+$ B-cells decreased from 14% to 10.8% (±2.2%) compared to unstimulated PBLs.

Since cells from different blood donors may vary in gene expression, we tested expression of TRPCs, TRPVs and TRPMs in individual donors and not in pooled cDNA templates. Fig. 2A shows the expression of TRPC1, C3 and C6, TRPV1 and V2, TRPM4 and M7 in all templates tested. Whereas TRPC1 and C3, TRPV1 and V2 and TRPM7 were consistently expressed in cells from all donors, mRNAs of TRPC6 and TRPM4 were expressed at varying levels in stimulated PBLs, but no expression was found in naïve $CD3^+$ T-cells. TRPC6 and TRPM4 were, however, clearly detectable in the two Jurkat T-cell lines, E6-1 and parental. TRPC4 and TRPC5 were neither found in unstimulated nor in stimulated PBLs nor in $CD3^+$ T-cells, but TRPC4 was strongly detectable in parental but not in E6-1 Jurkat T-cells. TRPC5 was faintly expressed in both Jurkat T-cell lines, parental and E6-1 (Fig. 2B). Our expression analysis of TRPC6 in Jurkat T-cells and PBLs is not consistent with the literature. In contrast to our results, Gamberucci et al. [41] found TRPC6 expression performing Western-Blot analysis in PHA/IL-2 stimulated PBL protein lysates. To confirm

Table 2
Expression of TRPs investigated by conventional RT-PCR.

	PBLs	Stim. PBLs	CD3$^+$	par	E6-1
TRPC1	8/8	4/4	5/5	1/1	1/1
TRPC2[a]	8/8	4/4	5/5	1/1	1/1
TRPC3	8/8	4/4	5/5	1/1	1/1
TRPC4	0/8 (P)	0/4 (P)	0/5	1/1	0/1
TRPC5	0/8 (P)	0/4 (P)	0/5 (P)	1/1	1/1
TRPC6	7/8	(1)/4	0/5	1/1	1/1
TRPC7	1/8	0/4 (P)	0/5 (P)	0/1	0/1
TRPV1	8/8	4/4	5/5	1/1	1/1
TRPV2	8/8	4/4	5/5	1/1	1/1
TRPV3	8/8	4/4	3/5	1/1	0/1
TRPV4	8/8	4/4	2/5	(1)/1	0/1
TRPV5	3/8	2/4	2/5	(1)/1	0/1
TRPV6	2/8	2/4	1/5	1/1	1/1
TRPM1	3/8	3/4	(3)/5	(1)/1	(1)/1
TRPM2	8/8	4/4	5/5	1/1	1/1
TRPM3	4/8	(1)/4	1/5	(1)/1	0/1
TRPM4	7/8	3 + (1)/4	0/5	1/1	1/1
TRPM5	8/8	4/4	2 + (1)/5	1/1	(1)/1
TRPM6	8/8	(3)/4	(1)/5	1/1	1/1
TRPM7	8/8	4/4	5/5	1/1	1/1
TRPM8	0/8 (P)	0/4 (P)	0/5 (P)	0/1	0/1

Expression of TRPs in peripheral blood lymphocytes (PBLs) (8 donors, PBLs), in stimulated PBLs (4 donors, stim. PBLs), T-cells (5 donors, CD3$^+$) and Jurkat T-cell lines (par and E6-1 ((#TIB-152, ATCC)) investigated by RT-PCR and confirmed by sequencing. P: cDNA of *n* donors (*n* as indicated) were pooled. Numbers in parenthesis indicate bands which were almost undetectable on the gel. [a]TRPC2 is a possible pseudogene in humans [42].

our results, we tested different primer pair combinations for TRPC6 in naïve CD3$^+$ T-cells (Fig. 2C). None of these combinations amplified a fragment of TRPC6, demonstrating that TRPC6 is not expressed in naïve CD3$^+$ T-cells.

Table 2 summarizes the expression of TRPs in PBLs, naïve CD3$^+$ T-cells, stimulated PBLs, and in Jurkat T-cell lines. Within the TRPC family, TRPC1 and TRPC3 are consistently expressed. The same is true for TRPC2 mRNA fragments, which is, however, known to be a pseudogene in humans [42]. TRPC4, C5, C6 and C7 were neither detectable in stimulated PBLs (except in one donor, see Table 2) nor in naïve CD3$^+$ T-cells. Within the TRPV subfamily, TRPV1 and V2, and within the TRPM subfamily, TRPM2 and TRPM7 were consistently expressed. TRPM8 was not found in any of the templates tested. The remaining members of the TRPV and TRPM family varied in the pattern and level of expression. The numbers in parentheses indicate expression of mRNA fragments at the limit of possible detection.

3.2. Regulation of expression of TRPs in effector CD4$^+$ T-cells following focal stimulation

CD4$^+$ T-cells play a central regulatory role in the adaptive immune system. Priming CD4$^+$ T-cell with an antigen-presenting cell triggers the stimulation and the subsequent differentiation from naïve to effector T-cells. Since the regulation of expression levels during these events might hint to a functional relevance of the affected genes, we analyzed the expression of different TRPs in CD4$^+$ T-cells following their stimulation. To address this, we negatively isolated CD4$^+$ T-cells from Ficoll-gradient purified PBLs to avoid any pre-stimulation of CD4$^+$ T-cells. Fig. 3A shows a representative image of anti-CD4 staining of isolated CD4$^+$ T-cells. The purity of the CD4$^+$ T-cell isolation was 96.8 ± 0.8% SD CD4$^+$ T-cells (840–1700 cells each donor) analyzed for the three different donors used for quantitative RealTime-PCR (qRT-PCR) analysis (see below). Instead of stimulation with antigen-presenting cells (APC), which would have had to be removed before RNA isolation (because they would contaminate qRT-PCR analysis), focal stimulation was

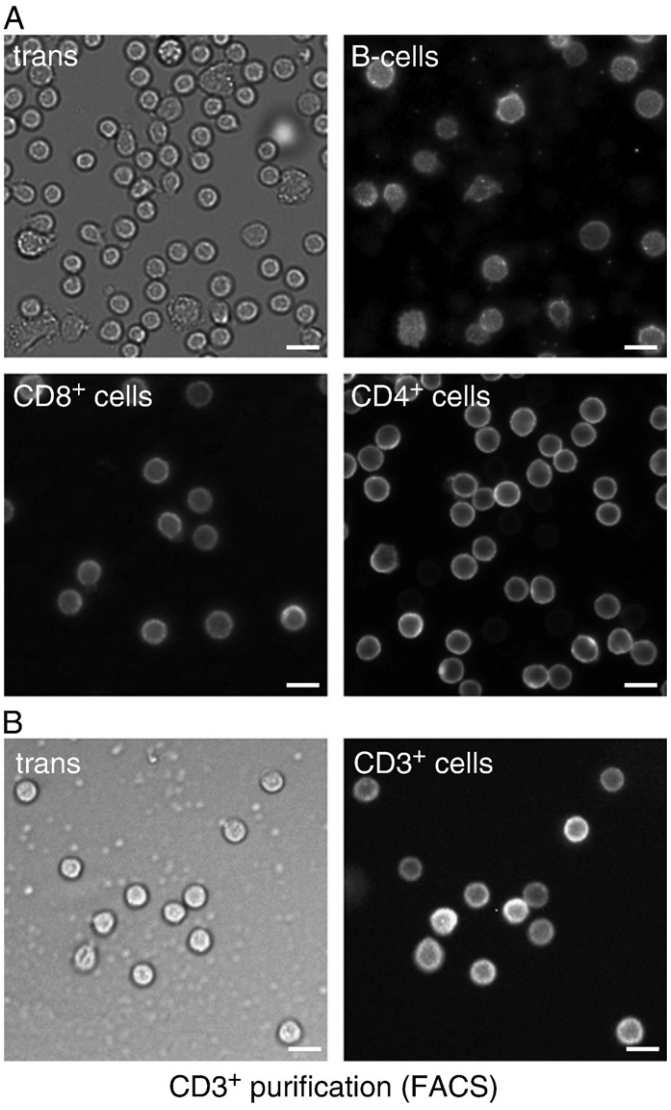

Fig. 1. Isolation of human PBLs and CD3$^+$ T-cells. A, PBL stained with antibodies against surface markers on B-cells (anti-CD19/FITC), CD8$^+$ T-cells (anti-CD8/RPE-Cy5) and CD4$^+$ T-cells (anti-CD4/RPE) after isolation from leukocyte reduction filters. B, Staining of CD3$^+$ T-cells (anti-CD3/FITC) following FACS sorting. Bars are 10 μm.

mimicked by anti-CD3/anti-CD28 coated beads as previously reported [38]. As shown in Fig. 3B, bead–cell contacts exist already after 7 h and were still present after 72 h. During stimulation, CD4$^+$ T-cells not only enlarged their size by a factor of 1.5 (Ø = 8.4 μm ± 0.6 for naïve cells (n = 380) versus 12.5 μm ± 1.1 (n = 76) for effector T-cells as analyzed in transmission images with TILL vision software) but also the amount of total RNA increased over 4 days by a factor of 6.2 ± 1.9 (n = 3). Rapid F-actin polymerization towards the T-cell-APC contact site is a hallmark of IS generation [43] and was observed at the CD4$^+$ T-cell-bead contact site (Fig. 3C) indicating formation of an immunological synapse. The functionality of T-cell stimulation with anti-CD3/anti-CD28 coated beads was also confirmed by up-regulation of IL-2R (CD25, [38]) and proliferation of T-cells (data not shown). Taken together, we conclude that CD4$^+$ T-cells are efficiently stimulated by antibody-coated beads with molecular and cellular consequences similar to the ones following stimulation by APC. Thus, we had appropriate starting material to investigate TRP expression following focal stimulation in CD4$^+$ T-cells.

Within the TRPC, TRPV and TRPM subfamilies, we analyzed the expression of TRPC1 and C3, TRPV1, TRPM2, M4 and M7 and in addition the expression of STIM1 and ORAI1 in antibody-coated bead

Table 3
Primer and PCR-conditions used for the quantitative RT-PCR.

Gene	Accession	Primer	Sequence 5′–3′	Ann. T.	Position (from start codon ATG)	Length of the PCR product
TRPC1	NM_003304,	forw	5′ tctggtatgaagggttggaa 3′	58 °C	1223–1242	139 bp
	ID:7220	rev	5′ tccttccgatcagcaaaatc 3′	58 °C	1342–1361	
TRPC3	NM_003305	forw	5′ ggaaggactgtaaaggaca 3′	56 °C	1711–1729	195 bp
	ID: 7222	rev	5′ cacaacggaagtcacttca 3′	56 °C	1887–1905	
TRPV1	AY131289	forw	5′ accacctggaacaccaacgt 3′	62 °C	2251–2270	178 bp
	ID: 7442	rev	5′ gctgagcagactgcctatct 3′	62 °C	2409–2428	
TRPM2	NM_003307	forw	5′ atgcctttggcgacatcgt 3′	58 °C	374–392	179 bp
	ID: 7226	rev	5′ cggcttcatgttgaagttct 3′	58 °C	533–552	
TRPM4	NM_017636	forw	5′ gtatctgctctcggacaag 3′	58 °C	1611–1629	160 bp
	ID: 54795	rev	5′ aagagctgaggaaactgcat 3′	58 °C	1751–1770	
TRPM7	NM_017672	forw	5′ ccagcaaatctaggagaaga 3′	58 °C	5380–5399	150 bp
	ID: 54822	rev	5′ caaatctgaaggctcatcct 3′	58 °C	5510–5529	
ORAI1	NM_032790	forw	5′ atgagcctcaacgagcact 3′	58 °C	190–218	160 bp
	ID: 84876	rev	5′ gtgggtagtcgtggtcag 3′	58 °C	332–349	
STIM1	NM_003156	forw	5′ cagagtctgcatgaccttca 3′	60 °C	766–785	125 bp
	ID: 6786	rev	5′ gcttcctgcttagcaaggtt 3′	60 °C	871–890	
RNAPol	NM_000937	forw	5′ ggagattgagtccaagttca 3′	58 °C	3208–3227	134 bp
	ID: 5430	rev	5′ gcagacacaccagcatagt 3′	58 °C	3323–3341	
TBP	NM_003194	forw	5′ cggagagttctgggattgt 3′	58 °C	467–485	161 bp
	ID: 6908	rev	5′ ggttcgtggctctcttatc 3′	58 °C	609–627	
HPRT1	NM_000194	forw	5′ caatgcagactttgctttcc 3′	58 °C	425–444	156 bp
	ID: 3251	rev	5′ caagggcatatcctacaaca 3′	58 °C	561–580	

stimulated $CD4^+$ T-cells over 13 days (Fig. 4 and Table 3). Relative expression of any gene of interest is expressed as $2^{-\Delta CT}$-values in relation to two different house keeping genes (HKG), TATA box binding protein (TBP) and RNA polymerase II (RNAPol). To show comparable expression levels, relative expression in naïve $CD4^+$ T-cells (0 days following stimulation, Fig. 4) was set to 1, except for TRPM4 and TRPC3. Since TRPM4 expression was not detectable at 7 h following stimulation and it was only detectable in one out of three donors in naïve $CD4^+$ T-cells and only in two out of three donors at 1 day following stimulation, the relative expression of TRPM4 was set to 1 two days following stimulation. For TRPC3, expression in naïve $CD4^+$ T-cells was only found in two donors, but expression level at 7 h following stimulation was highly comparable to the level of naïve cells. For that reason relative expression at 7 h was set to 1. Among the TRPs analyzed, most of them remained constant at their RNA expression level over time. Only the expressions of TRPC3 and TRPM2 were strongly regulated over time compared to naïve $CD4^+$ T-cells, but with different kinetics (Fig. 4). Seven and twenty-four hours following stimulation, TRPC3 mRNA levels were almost identical in naïve $CD4^+$ T-cells. Up-regulation of TRPC3 mRNA was observed from day 1 to days 4–5 following stimulation, which represents the time window during which naïve $CD4^+$ T-cell develop into effector T-cells (up-regulation of IL-2R, down-regulation of CD62 and IL-2 secretion, [38]). The cells showed enlarged cell sizes (see above) and the amount of total RNA was increased by a factor of around 6 ($n=3$). In contrast, TRPM2 mRNA was first down-regulated (by a factor of 6 at 7 h following stimulation), and slightly increased until day 3 (factor of 1.7 at day 3) but was than up-regulated by a factor of around 7–8 until day 6 following stimulation. The up-regulation of TRPM2 at later time points (4 to 6 days following stimulation) may represent a mechanism to control survival or death of individual effector T-cells, because TRPM2 activation by extracellular signals as oxidative stress, H_2O_2 and TNF-α can induce apoptosis [44].

The insets in Fig. 4 show that the relative expression levels of TRPC1, TRPV1 and STIM1 were first down-regulated compared to the level of naïve T-cells, but reached the same level or slightly higher levels at day 2 to day 5 following stimulation. TRPM4 mRNA was only consistently expressed after 2 days of stimulation, but expression levels increased until days 4–5 (up to a factor of 3.4, mean of the relative expression to both house keeping genes). Compared to this level of regulation, the expression of TRPM7 and ORAI1 mRNAs remained stable over time. The most abundant TRP channel is TRPM7 in $CD4^+$ T-cells. In addition, TRPV1 and TRPV2 (data not shown) have an almost comparable expression level. TRPC1 is slightly less expressed than TRPV1 (for original CT values see figure legend of Fig. 4). TRPC3 expression is low under resting conditions but is several fold up-regulated following stimulation with antibody coated beads. Regulation of expression is summarized in Table 4.

3.3. Down-regulation of TRPC3 reduces proliferation of $CD4^+$ T-cells

Since TRPC3 was found to be up-regulated during T-cell activation (Fig. 4) and since it was reported to contribute to Ca^{2+} entry following TCR stimulation [45], we analyzed its potential function using an siRNA approach. As a positive control for the siRNA technology in primary human $CD4^+$ T-cells, we used siRNAs against STIM1. The role of STIM1 for Ca^{2+} entry has been clearly established as an activator for store-operated CRAC/ORAI channels. We found the efficiency of STIM1 siRNA down-regulation to be in the range of 50% on mRNA level (Supplementary Fig. 1A). To investigate the functional relevance of STIM1 down-regulation, we analyzed Ca^{2+} influx in siRNA transfected effector $CD4^+$ T-cells following depletion of the intracellular stores by thapsigargin (TG) and the re-addition of 0.25 mM Ca^{2+} (Supplementary Fig. 1B). Ca^{2+} influx rates were reduced by 54% in STIM1 siRNA transfected $CD4^+$ T-cells compared to control cells. Interestingly, not only Ca^{2+} influx was affected but resting $[Ca^{2+}]_i$ was also reduced to about 50% in STIM1 siRNA transfected naïve $CD4^+$ T-cells (Supplementary Fig. 1C, 6 days following transfection, without stimulation). Resting Ca^{2+} levels were, however, not reduced in stimulated cells treated with STIM1 siRNA (compare initial Ca^{2+} levels in Supplementary Fig. 1B) while CRAC influx was clearly reduced. The reduction of resting Ca^{2+} in unstimulated naïve T-cells indicates that very few if any CRAC channels are activated under these conditions. Ca^{2+} stores are not emptied under these conditions indicating further that CRAC channels should not be active. The reduction of resting Ca^{2+} in naïve T-cells thus suggests that CRAC is not the only Ca^{2+} influx pathway controlling resting Ca^{2+} levels in T-cells.

To analyze the time dependence of STIM siRNA down-regulation, we have investigated Ca^{2+}-signals on days 1–3 after T-cell

stimulation. Whereas Ca^{2+}-signals were reduced on days 1 and 2, this was not the case on day 3 as shown in the examples and the statistics of the Ca^{2+}-influx slope and the Ca^{2+} plateau (Supplementary Fig. 2A,

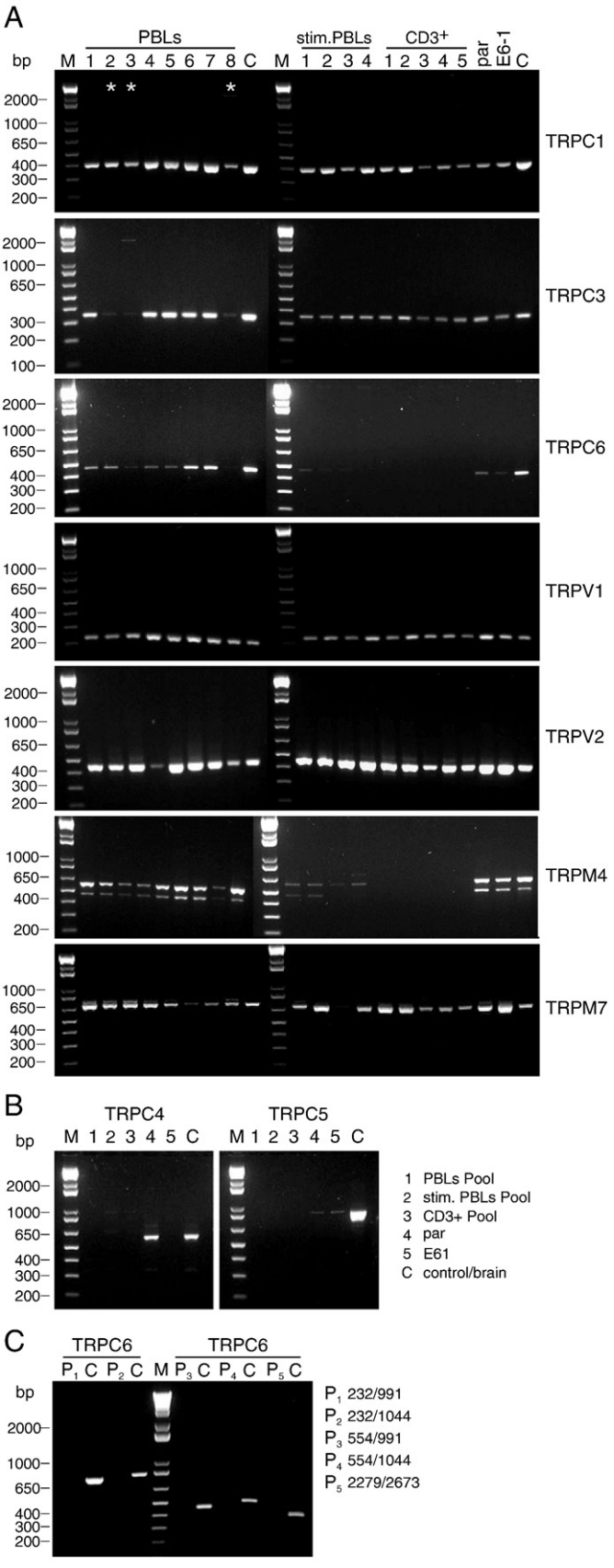

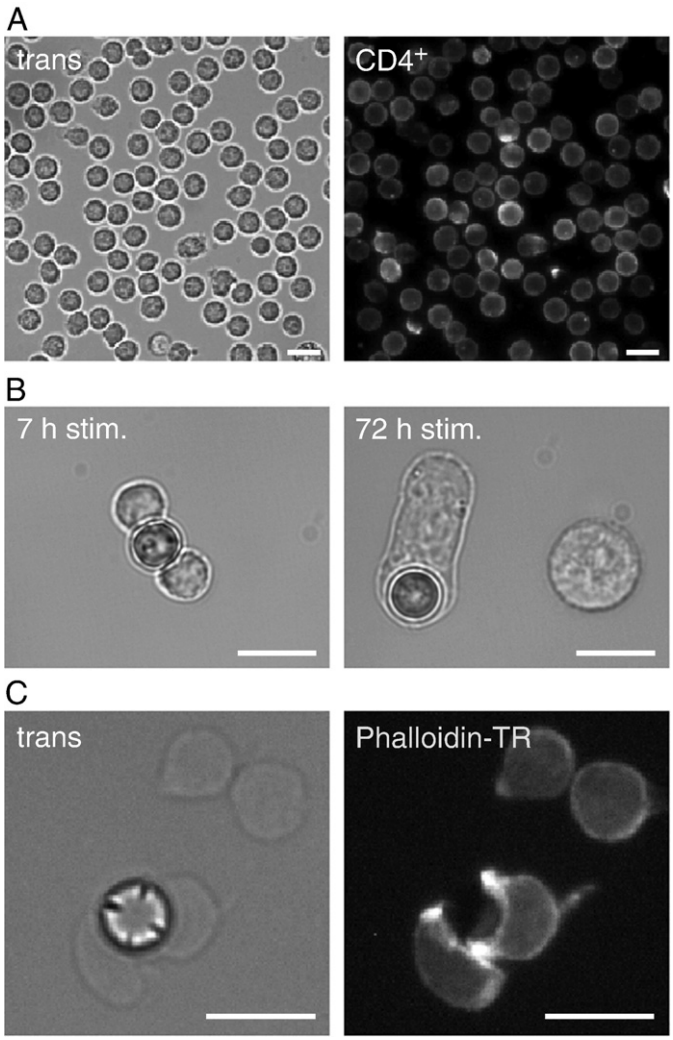

Fig. 3. Focal stimulation of $CD4^+$ T-cells with anti-CD3/anti-CD28 coated beads. A, Staining of negatively isolated $CD4^+$ T-cells (anti-CD4/RPE) illustrate the purity of the isolation procedure (96%-97%, see text). B, Trans-illumination images show $CD4^+$ T-cells in contact with antibody-coated beads following 7 (left) and 72 h (right). C, Staining of the F-actin cytoskeleton with phalloidin-TexasRed (Phalloidin-TR) demonstrates the rearrangement of the F-cytoskeleton towards the contact site between a bead and a cell. Bars are 10 μm.

B). This finding correlates well with STIM1 mRNA down-regulation analyzed by qRT-PCR with the level of mRNA already recovering after 2 days of stimulation (Supplementary Fig. 2C). Subsequently, we investigated the effect of STIM1 down-regulation in proliferation experiments, because proliferation is Ca^{2+}-dependent. As expected, STIM1 siRNA transfected $CD4^+$ T-cells proliferate less compared to those transfected with control siRNA (Supplementary Fig. 1D).

Next, we analyzed TRPC3 function following the transfection of $CD4^+$ T-cells with TRPC3 siRNA. Fig. 5A illustrates the efficiency of down-regulation in primary $CD4^+$ T-cells (64.4% reduction at day 2,

Fig. 2. Expression analysis of TRPCs, TRPVs and TRPMs in primary human PBLs, $CD3^+$ T-cells and Jurkat T-cell lines, E6-1 and parental. A, Expression pattern of TRPs in unstimulated PBLs (8 donors), stimulated PBLs (4 donors), $CD3^+$ T-cells (5 donors) and Jurkat T-cell lines parental (par) and E6-1 was analyzed by conventional RT-PCR. Stars indicate templates prepared from mRNA which lead to weaker signals compared to templates reverse transcribed from total RNA. B, Expression analysis of TRPC4 and TRPC5 were carried out within the same templates used in A, but templates of single donors were pooled. C, Expression analysis of TRPC6 in $CD3^+$ T-cells (5 donors pooled) with 5 different primer pairs (P_1–P_5). Templates (C) from human brain (for TRPCs, TRPV1 and V2, TRPM7) and colon (for TRPM4) were used as positive controls. For details of PCR conditions see also Table 1.

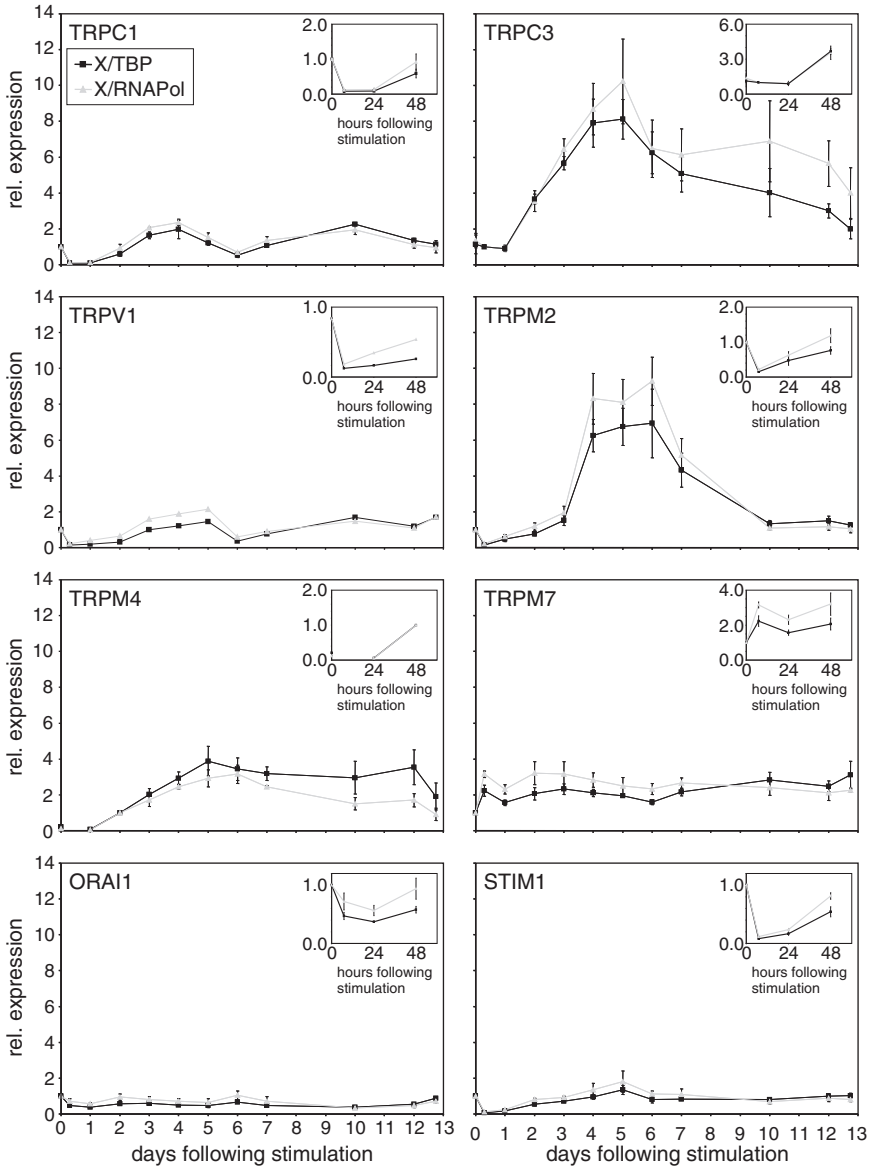

Fig. 4. Expression analysis of TRPs in CD4$^+$ T-cells over 13 days. The relative expression ($2^{-\Delta CT}$ values) of TRPC1, TRPC3, TRPV1, TRPM2, TRPM4 and TRPM7, ORAI1 and STIM1 were analyzed in three different donors of CD4$^+$ T-cells over 13 days. Time point 0 corresponds to naïve CD4$^+$ T-cells that were stimulated with anti-CD3/anti-CD28 coated beads. Expression of the gene of interest was normalized to the expression of two different house keeping genes TATA box-binding protein (black rectangle) and RNA Polymerase II (grey triangle). Data points are presented as means ± SEM of three different donors. Expression at time point 0 was set to 1, except for TRPC3 (expression at 7 h was set to 1) and for TRPM4 (expression at 48 h was set to 1) due to missing detectable CT values in all of the three donors (corresponding to no expression or expression under the detection level) at earlier time points. Insets show relative expression levels from 0 to 48 h. Absolute levels of expression (= original CT values without including any reference genes) in naïve CD4$^+$ T-cells are: 26.4 ± 0.3 (TRPC1); 35.2 ± 1.4 (TRPC3); 24.6 (TRPV1); 28.6 ± 0.7 (TRPM2); 33.0 (TRPM4); 22.2 ± 0.4 (TRPM7), 20.7 ± 0.5 (ORAI1); 20.5 ± 0.3 (STIM1).

60.7% reduction at day 3 in TRPC3 siRNA (C3-1mod) transfected compared to control siRNA transfected CD4$^+$ T-cells). The TRPC3 siRNA was also analyzed in HEK-293 over-expressing TRPC3 cells (54% reduction in TRPC3 siRNA transfected compared to control siRNA transfected HEK-293 cells, Supplementary Fig. 3). To analyze the potential role of TRPC3 in the Ca^{2+} homeostasis of CD4$^+$ T-cells, we first investigated whether Ca^{2+} influx was changed in TRPC3 siRNA transfected cells compared to control cells (transfected with control siRNA). However, we did not see a significant difference when Ca^{2+} stores were depleted with thapsigargin (Fig. 5B) which is in agreement with [45] and [26]. Ca^{2+} influx rates were 4.0 nM $Ca^{2+}/s \pm 0.2$ in control siRNA transfected T-cells ($n = 1303$) similar to 3.8 nM $Ca^{2+}/s \pm 0.3$ in TRPC3 siRNA transfected T-cells ($n = 1046$). The Ca^{2+} plateau was 100.8 nM $Ca^{2+} \pm 2.5$ in control siRNA transfected T-cells ($n = 1303$) versus 102.6 nM $Ca^{2+} \pm 2.9$ in TRPC3 siRNA transfected T-cells ($n = 1046$). However, we found a reduction of about 20% in the resting $[Ca^{2+}]_i$ levels in naïve CD4$^+$ T-cells 6 days after transfection (Fig. 5C). In addition, we also observed a reduction of $[Ca^{2+}]_i$ in anti-CD3/anti-CD28-coated bead-stimulated CD4$^+$ T-cells under Ca^{2+}-limiting conditions (Fig. 5D). A significant difference in the Ca^{2+}-signals was measured with 36 or 56 μM external Ca^{2+} present. Similarly, we observed a reduction of proliferation in TRPC3 siRNA transfected CD4$^+$ T-cells stimulated with anti-CD3/anti-CD28 coated beads under Ca^{2+}-limiting conditions within the same range (Fig. 5E).

3.4. Conclusions

Very little information is available about the expression of TRP proteins in primary human T-cells. We found the TRP expression

Table 4
Regulation of expression in anti-CD3/CD28 coated bead stimulated CD4$^+$ T-cells over 14 days.

	Regulation of expression in anti-CD3/CD28 coated bead stimulated CD4$^+$ T-cells over 13 days
TRPC1	+/−
TRPC3	++[b]
TRPV1[a]	+/−
TRPM2	++
TRPM4	+[c]
TRPM7	+/−
ORAI1	+/−
STIM1	+/−

The regulation of expression of TRPs, ORAI1 and STIM1 were analyzed in anti-CD3/CD28 coated bead stimulated CD4$^+$ T-cells by quantitative RT-PCR. Expression was analyzed as relative expression to two different house-keeping genes (TATA box binding protein and RNA Polymerasell A, compare Fig. 4) in three different donors. +/−: no or only slight regulation; +: upregulation up to 5-fold; ++ upregulation up to 10-fold.
[a] Expression was investigated in only one donor.
[b] Expression at 7 h was set to 1.
[c] Expression at 2 days (48 h) was set to 1.

profile of primary human T-cells to be significantly different from Jurkat T-cell lines. Among the TRP mRNAs of the TRPC, TRPM, and TRPV family, we found consistent expression of TRPC1, TRPC3, TRPV1, TRPM2, and TRPM7 in primary human CD4$^+$ T-cells. Among these, TRPC3 and TRPM2 were strongly up-regulated following focal stimulation of CD4$^+$ T-cells, but with different kinetics. We found that down-regulation of TRPC3 with siRNA moderately reduced proliferation of primary CD4$^+$ T-cells. In parallel, resting Ca^{2+} in CD4$^+$ T-cells was also reduced.

4. Discussion

In contrast to murine tissues, murine cells, and T-cell lines, in which expression data of TRP proteins or mRNA have been published [46–48], very little information is available about the expression of TRP proteins in human T-cells. We have analyzed the expression of the TRPC, TRPV and TRPM subfamilies in primary peripheral blood lymphocytes, unstimulated and stimulated, CD3$^+$ T-cells and the commonly used Jurkat T-cell lines parental and E6-1. In addition, we have investigated the regulation of TRPC1 and C3, TRPV1, TRPM2, M4 and M7 and ORAI1 and STIM1 following focal stimulation with antibody coated beads by qRT-PCR in CD4$^+$ T-cells.

Within the TRPV family, we found TRPV1 and V2 highly and consistently expressed in all cell types analyzed whereas the expression of TRPV3, V4, V5 and V6 differed in CD3$^+$ T-cells between the donors. For instance, TRPV6 was only detected in one donor out of five which is maybe due to expression levels close to the detection limit, but expression was found in both Jurkat T-cell lines. Others have detected TRPV1, V2, V3 and V4 in human leukocytes [49] and TRPV5 and V6 in primary T-cells using RT-PCR [50], but TRPV6 could not be found with Northern blot technology in human leukocytes [51]. Taken together with our expression data, it is questionable if TRPV3, V4, V5 and V6 play a prominent role in primary CD3$^+$ T-cells. TRPV1 as well as TRPV2 are involved in pain and heat sensation [52], but only very little information is available about their function in cells of the immune system. In dendritic cells, capsaicin activates TRPV1 and is involved in the immune responses [53].

Within the TRPM family, only TRPM2 and TRPM7 were consistently expressed in PBLs and T-cells. TRPM4 was not detectable in naïve T-cells but in effector CD4$^+$ T-cells and in Jurkat T-cell lines, which is consistent with the literature [48,54–56]. Only after 48 h of stimulation, TRPM4 was expressed in CD4$^+$ T-cells in all three donors investigated. Since TRPM4 is a Ca^{2+} activated non-selective cation channel, TRPM4 might depolarize the membrane potential in activated T-cells through Na^+ influx, thus preventing a Ca^{2+} overload in these cells [57,58]. TRPM2 expression was highly increased 4 days after stimulation but already stably expressed in naïve T-cells (see Fig. 4 and Table 2). Whether TRPM2, which is activated by intracellular Ca^{2+} [59] and by H_2O_2 [60], has different physiological functions in naïve or in effector T-cells is not yet clear.

The published expression data of TRPCs in Jurkat T-cells is contradictory [41,45,48,61]. We found that the expression pattern of the TRPC subfamily in primary human T-cells differs significantly from the expression in T-cell lines. We found only TRPC1 and TRPC3 to be consistently expressed and no expression of TRPC4, C5, C6 and C7 in primary CD3$^+$ T-cells, which is different from the expression pattern in the Jurkat cell lines. Due to this discrepancy, one has to be cautious when using T-cell lines (and probably other cell lines) as a model to study TRPC channel function.

Using qRT-PCR, we showed that TRPC3 is highly up-regulated in CD4$^+$ T-cells stimulated with anti-CD3/anti-CD28 coated beads compared to naïve T-cells whereas TRPC1 and ORAI1 expression remains almost constant. It has been shown that TRPC1 and TRPC3 channels can assemble in heteromeric complexes [62]. In addition, STIM1 was shown to directly activate TRPC1 and indirectly TRPC3 by mediating heteromultimerization of TRPC1 with TRPC3 [63]. We found that both, STIM1 and TRPC3 down-regulation, reduced resting intracellular [Ca^{2+}] in naïve CD4$^+$ T-cells and cell proliferation. However, the effect of STIIM1 siRNA down-regulation was more dramatic than that of TRPC3. This is not surprising, as STIM1 is a key player of SOCE [8,9] and TRPC3 is not involved in SOCE [26,45, in agreement with our results]. The mode of TRPC3 activation is unclear but appears to be downstream of TCR stimulation [45] and PLC activation (reviewed in [30]).

We only observed the TRPC3 effect on proliferation under Ca^{2+} limiting conditions. Since ORAI1 channels are of course dominating Ca^{2+} signals in T-cells [17], ORAI1 alone is usually sufficient to mediate the Ca^{2+} influx required for proliferation. Under highly Ca^{2+} limiting conditions, even the small Ca^{2+} influx through TRPC3 channels might be required to drive proliferation. In addition, proliferation depends on cytosolic resting Ca^{2+} concentrations analyzed over several days [38] under these conditions. Since TRPC3 reduces the resting Ca^{2+} concentration, the subsequent reduction of proliferation was expected. How TRPC3 contributes to Ca^{2+} entry in T-cells is presently not clear. There are at least three different possibilities:

1. TRPC3 activity generates Ca^{2+} entry by itself. This happens at the cost of very high Na^+ entry and T-cell polarization because TRPC3 channels are considered to be non-selective cation channels.
2. A close association between TRPC3 and the Na^+/Ca^{2+} exchanger (NCX) as described for HEK-293 [37] could explain TRPC3 dependent Ca^{2+} entry if Na^+ entry through TRPC3 drives NCX in the reverse mode. However there is no evidence for NXC activity in T-cells [64].
3. There is some evidence that members of the TRPC family can interact with STIM and ORAI proteins thus influencing SOCE [63]. We have, however, never found a hint that TRPC3 is activated by store depletion [45], however we can not exclude this possibility. Ong et al. [27] described a ternary complex of TRPC1, STIM1 and ORAI1 and reported that it was required for SOCE. In pull-down assays, it was shown that TRPC3 and TRPC6 physically interact with ORAI1, and ORAI1 was shown to enhance SOCE in TRPC3 or TRPC6 expressing HEK-293 cells [65]. Very recently, a model was proposed that ORAI:TRPC complexes, depending on their localization in or outside lipid rafts, mediate SOCE or ROCE [66,67]. Given the dominating importance of the STIM-ORAI dependent Ca^{2+} entry in T-cells, one has to be careful to assign premature functions for TRPC channels in T-cells. Yet, its regulation makes TRPC3 an interesting candidate to contribute to Ca^{2+} signaling in T-cells.

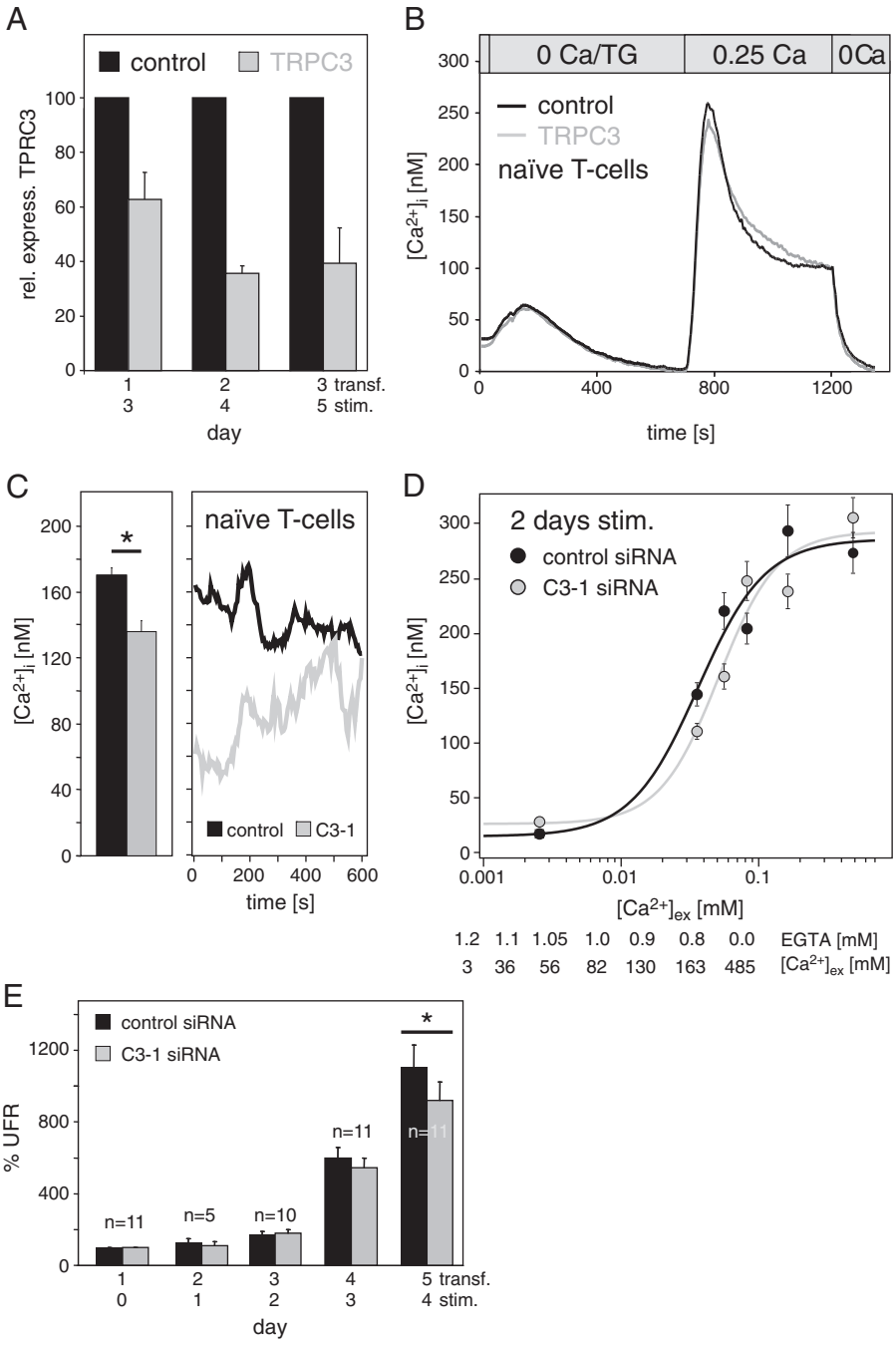

Fig. 5. Analysis of TRPC3 function in CD4$^+$ T-cells with small interfering RNAs (siRNAs). A, TRPC3 is down-regulated in primary TRPC3 siRNA transfected CD4$^+$ T-cells. Cells were stimulated for 2 days and TRPC3 expression was investigated 1 to 3 days after transfection (TRPC3 siRNAmod (TRPC3, grey); non-silencing, control siRNA (control, black)). TRPC3 expression was calculated relative to the mean of three house-keeping genes TBP, RNAPolymerase II and hypoxanthine phosphoribosyltransferase 1 (HPRT1). Relative expression in control cells was set to 100%. B, Ca^{2+} influx was not affected in naïve TRPC3 siRNAmod (TRPC3, grey) compared to control siRNA (control, black) transfected CD4$^+$ T-cells when stimulated with thapsigargin. Naïve cells (not bead-stimulated) were measured 4 days after transfection. C, Analysis of intracellular Ca^{2+} ($[Ca^{2+}]_i$) under Ca^{2+}-limiting conditions in siRNA transfected, naïve CD4$^+$ T-cells. Resting Ca^{2+} is reduced in TRPC3 siRNA transfected CD4$^+$ T-cells (C3-1, grey, $n=87$) compared to control siRNA transfected CD4$^+$ T-cells (black, control, $n=247$) 6 days following transfection by 20% (cells of two different donors, measured in complete AIMV medium). Bars show means ± SEM, $p<0.001$ calculated over the complete experiment of 600 s. Traces show a representative cell of each TRPC3 siRNA (grey) and control siRNA transfected CD4$^+$ T-cells (black). D, Extracellular $[Ca^{2+}]$ ($[Ca^{2+}]_{ex}$) was reduced by the addition of EGTA and corresponding $[Ca^{2+}]$ within the medium were determined as described [38]. Final [EGTA] added to the medium and ($[Ca^{2+}]_{ex}$) are given in the table (below). CD4$^+$ T-cells were stimulated for 2 days with anti-CD3/anti-CD28 antibody-coated beads 4 days after transfection with either TRPC3 siRNA (grey) or control siRNA (black). Circles show the mean ± SEM of 38 to 138 cells of two different donors. E, Proliferation of TRPC3 siRNA (C3-1, grey) was reduced compared to control siRNA (black) transfected CD4$^+$ T-cells at day 4 following stimulation with anti-CD3/anti-CD28 coated beads. Proliferation was measured under Ca^{2+} limiting conditions (addition of 1.1 mM EGTA corresponding to 46 μM free extracellular $[Ca^{2+}]$ [38]) 1 to 5 days after transfection corresponding to days 0, 1, 2, 3 and 4 after stimulation. Relative fluorescence units (RFU) at day 0 were set to 100% and data are shown as means ± SEM, numbers of donors (n) are indicated. At day 4, reduction in proliferation was about 10% ($p=0.04$).

EGTA [mM]	1.2	1.1	1.05	1.0	0.9	0.8	0.0
$[Ca^{2+}]_{ex}$ [mM]	3	36	56	82	130	163	485

Acknowledgments

Research carried out for this study with human material (leukocyte reduction filters from human blood donors) is authorized by the local ethic committee (declaration of no objection from 5.4.2005 (Prof. Schie/Gn)). We are very grateful to Mike Zhu for providing TRPC3 stably expressing TRPC3 HEK-293 cells. We also thank members of the Department of Molecular Cell Biology (in

particular Peter Lipp, Gregor Reither and Achim Heinz) for helping with quantitative RealTime PCR, providing the MX3000 instrument and the software to analyze RealTime PCR results in IgorPro. We thank Stephan E. Philipp for purifying $CD3^+$ T-cells by FACS and Ulrich Wissenbach for providing mRNA from placenta. This project was funded by the Deutsche Forschungsgemeinschaft (SFB 530, project A3, and the Graduate Colleges GK377 and GK845, to M Hoth) and two competitive research grants from the Saarland University (HOMFOR and ZFK, both to EC Schwarz).

All authors concurred with the submission and the material submitted for publication has not been previously reported and is not under consideration for publication elsewhere.

The authors have no conflicting financial interests.

Appendix A. Supplementary data

Supplementary data to this article can be found online at doi:10.1016/j.bbamcr.2010.12.022.

References

[1] J. Jacobelli, P.G. Andres, J. Boisvert, M.F. Krummel, New views of the immunological synapse: variations in assembly and function, Curr. Opin. Immunol. 16 (2004) 345–352.
[2] P. Friedl, A.T. den Boer, M. Gunzer, Tuning immune responses: diversity and adaptation of the immunological synapse, Nat. Rev. Immunol. 5 (2005) 532–545.
[3] S. Feske, Calcium signalling in lymphocyte activation and disease, Nat. Rev. Immunol. 7 (2007) 690–702.
[4] A. Lanzavecchia, F. Sallusto, Antigen decoding by T lymphocytes: from synapses to fate determination, Nat. Immunol. 2 (2001) 487–492.
[5] G.R. Crabtree, E.N. Olson, NFAT signaling: choreographing the social lives of cells, Cell 109 (Suppl) (2002) S67–S79.
[6] R.T. Abraham, A. Weiss, Jurkat T cells and development of the T-cell receptor signalling paradigm, Nat. Rev. Immunol. 4 (2004) 301–308.
[7] M. Hoth, R. Penner, Depletion of intracellular calcium stores activates a calcium current in mast cells, Nature 355 (1992) 353–356.
[8] J. Liou, M.L. Kim, W.D. Heo, J.T. Jones, J.W. Myers, J.E. Ferrell Jr., T. Meyer, STIM is a Ca2+ sensor essential for Ca2+-store-depletion-triggered Ca2+ influx, Curr. Biol. 15 (2005) 1235–1241.
[9] J. Roos, P.J. DiGregorio, A.V. Yeromin, K. Ohlsen, M. Lioudyno, S. Zhang, O. Safrina, J.A. Kozak, S.L. Wagner, M.D. Cahalan, G. Velicelebi, K.A. Stauderman, STIM1, an essential and conserved component of store-operated Ca2+ channel function, J. Cell Biol. 169 (2005) 435–445.
[10] S. Feske, Y. Gwack, M. Prakriya, S. Srikanth, S.H. Puppel, B. Tanasa, P.G. Hogan, R.S. Lewis, M. Daly, A. Rao, A mutation in Orai1 causes immune deficiency by abrogating CRAC channel function, Nature 441 (2006) 179–185.
[11] M. Vig, C. Peinelt, A. Beck, D.L. Koomoa, D. Rabah, M. Koblan-Huberson, S. Kraft, H. Turner, A. Fleig, R. Penner, J.P. Kinet, CRACM1 is a plasma membrane protein essential for store-operated Ca2+ entry, Science 312 (2006) 1220–1223.
[12] S.L. Zhang, A.V. Yeromin, X.H. Zhang, Y. Yu, O. Safrina, A. Penna, J. Roos, K.A. Stauderman, M.D. Cahalan, Genome-wide RNAi screen of Ca(2+) influx identifies genes that regulate Ca(2+) release-activated Ca(2+) channel activity, Proc. Natl Acad. Sci. USA 103 (2006) 9357–9362.
[13] R.M. Luik, M.M. Wu, J. Buchanan, R.S. Lewis, The elementary unit of store-operated Ca2+ entry: local activation of CRAC channels by STIM1 at ER-plasma membrane junctions, J. Cell Biol. 174 (2006) 815–825.
[14] P.B. Stathopulos, G.Y. Li, M.J. Plevin, J.B. Ames, M. Ikura, Stored Ca2+ depletion-induced oligomerization of stromal interaction molecule 1 (STIM1) via the EF-SAM region: an initiation mechanism for capacitive Ca2+ entry, J. Biol. Chem. 281 (2006) 35855–35862.
[15] J. Liou, M. Fivaz, T. Inoue, T. Meyer, Live-cell imaging reveals sequential oligomerization and local plasma membrane targeting of stromal interaction molecule 1 after Ca2+ store depletion, Proc. Natl Acad. Sci. USA 104 (2007) 9301–9306.
[16] W.I. DeHaven, B.F. Jones, J.G. Petranka, J.T. Smyth, T. Tomita, G.S. Bird, J.W. Putney Jr., TRPC channels function independently of STIM1 and Orai1, J. Physiol. 587 (2009) 2275–2298.
[17] S. Feske, M. Prakriya, A. Rao, R.S. Lewis, A severe defect in CRAC Ca2+ channel activation and altered K+ channel gating in T cells from immunodeficient patients, J. Exp. Med. 202 (2005) 651–662.
[18] R.S. Lewis, Calcium signaling mechanisms in T lymphocytes, Annu. Rev. Immunol. 19 (2001) 497–521.
[19] R.M. Luik, R.S. Lewis, New insights into the molecular mechanisms of store-operated Ca2+ signaling in T cells, Trends Mol. Med. 13 (2007) 103–107.
[20] M.K. Jha, A. Badou, M. Meissner, J.E. McRory, M. Freichel, V. Flockerzi, R.A. Flavell, Defective survival of naive CD8+ T lymphocytes in the absence of the beta3 regulatory subunit of voltage-gated calcium channels, Nat. Immunol. 10 (2009) 1275–1282.
[21] A. Badou, M.K. Jha, D. Matza, W.Z. Mehal, M. Freichel, V. Flockerzi, R.A. Flavell, Critical role for the beta regulatory subunits of Cav channels in T lymphocyte function, Proc. Natl Acad. Sci. USA 103 (2006) 15529–15534.
[22] L. Birnbaumer, The TRPC class of ion channels: a critical review of their roles in slow, sustained increases in intracellular Ca2+ concentrations, Annu. Rev. Pharmacol. Toxicol. 49 (2009) 395–426.
[23] I. Jardin, L.J. Gomez, G.M. Salido, J.A. Rosado, Dynamic interaction of hTRPC6 with the Orai1-STIM1 complex or hTRPC3 mediates its role in capacitative or noncapacitative Ca(2+) entry pathways, Biochem. J. 420 (2009) 267–276.
[24] G.M. Salido, S.O. Sage, J.A. Rosado, TRPC channels and store-operated Ca(2+) entry, Biochim. Biophys. Acta 1793 (2009) 223–230.
[25] J.P. Yuan, M.S. Kim, W. Zeng, D.M. Shin, G. Huang, P.F. Worley, S. Muallem, TRPC channels as STIM1-regulated SOCs, Channels (Austin) 3 (2009).
[26] S. Brechard, C. Melchior, S. Plancon, V. Schenten, E.J. Tschirhart, Store-operated Ca2+ channels formed by TRPC1, TRPC6 and Orai1 and non-store-operated channels formed by TRPC3 are involved in the regulation of NADPH oxidase in HL-60 granulocytes, Cell Calcium 44 (2008) 492–506.
[27] H.L. Ong, K.T. Cheng, X. Liu, B.C. Bandyopadhyay, B.C. Paria, J. Soboloff, B. Pani, Y. Gwack, S. Srikanth, B.B. Singh, D.L. Gill, I.S. Ambudkar, Dynamic assembly of TRPC1-STIM1-Orai1 ternary complex is involved in store-operated calcium influx. Evidence for similarities in store-operated and calcium release-activated calcium channel components, J. Biol. Chem. 282 (2007) 9105–9116.
[28] M. Trebak, L. Lemonnier, J.T. Smyth, G. Vazquez, J.W. Putney Jr., Phospholipase C-coupled receptors and activation of TRPC channels, Handb. Exp. Pharmacol. (2007) 593–614.
[29] K. Venkatachalam, C. Montell, TRP channels, Annu. Rev. Biochem. 76 (2007) 387–417.
[30] A. Dietrich, M. Mederos y Schnitzler, H. Kalwa, U. Storch, T. Gudermann, Functional characterization and physiological relevance of the TRPC3/6/7 subfamily of cation channels, Naunyn Schmiedebergs Arch. Pharmacol. 371 (2005) 257–265.
[31] X. Liu, K.T. Cheng, B.C. Bandyopadhyay, B. Pani, A. Dietrich, B.C. Paria, W.D. Swaim, D. Beech, E. Yildrim, B.B. Singh, L. Birnbaumer, I.S. Ambudkar, Attenuation of store-operated Ca2+ current impairs salivary gland fluid secretion in TRPC1(−/−) mice, Proc. Natl Acad. Sci. USA 104 (2007) 17542–17547.
[32] M.S. Kim, J.H. Hong, Q. Li, D.M. Shin, J. Abramowitz, L. Birnbaumer, S. Muallem, Deletion of TRPC3 in mice reduces store-operated Ca2+ influx and the severity of acute pancreatitis, Gastroenterology 137 (2009) 1509–1517.
[33] A. Riccio, Y. Li, J. Moon, K.S. Kim, K.S. Smith, U. Rudolph, S. Gapon, G.L. Yao, E. Tsvetkov, S.J. Rodig, A. Van't Veer, E.G. Meloni, W.A. Carlezon Jr., V.Y. Bolshakov, D.E. Clapham, Essential role for TRPC5 in amygdala function and fear-related behavior, Cell 137 (2009) 761–772.
[34] W.A. Large, S.N. Saleh, A.P. Albert, Role of phosphoinositol 4, 5-bisphosphate and diacylglycerol in regulating native TRPC channel proteins in vascular smooth muscle, Cell Calcium 45 (2009) 574–582.
[35] P. Eder, D. Probst, C. Rosker, M. Poteser, H. Wolinski, S.D. Kohlwein, C. Romanin, K. Groschner, Phospholipase C-dependent control of cardiac calcium homeostasis involves a TRPC3-NCX1 signaling complex, Cardiovasc. Res. 73 (2007) 111–119.
[36] M. Goel, C.D. Zuo, W.G. Sinkins, W.P. Schilling, TRPC3 channels colocalize with Na+/Ca2+ exchanger and Na+ pump in axial component of transverse-axial tubular system of rat ventricle, Am. J. Physiol. Heart Circ. Physiol. 292 (2007) H874–H883.
[37] C. Rosker, A. Graziani, M. Lukas, P. Eder, M.X. Zhu, C. Romanin, K. Groschner, Ca(2+) signaling by TRPC3 involves Na(+) entry and local coupling to the Na(+)/Ca(2+) exchanger, J. Biol. Chem. 279 (2004) 13696–13704.
[38] E.C. Schwarz, C. Kummerow, A.S. Wenning, K. Wagner, A. Sappok, K. Waggershauser, D. Griesemer, B. Strauss, M.J. Wolfs, A. Quintana, M. Hoth, Calcium dependence of T cell proliferation following focal stimulation, Eur. J. Immunol. 37 (2007) 2723–2733.
[39] C.M. Fanger, M. Hoth, G.R. Crabtree, R.S. Lewis, Characterization of T cell mutants with defects in capacitative calcium entry: genetic evidence for the physiological roles of CRAC channels, J. Cell Biol. 131 (1995) 655–667.
[40] S. Rozen, H. Skaletsky, Primer3 on the WWW for general users and for biologist programmers, Meth. Mol. Biol. 132 (2000) 365–386.
[41] A. Gamberucci, E. Giurisato, P. Pizzo, M. Tassi, R. Giunti, D.P. McIntosh, A. Benedetti, Diacylglycerol activates the influx of extracellular cations in T lymphocytes independently of intracellular calcium-store depletion and possibly involving endogenous TRP6 gene products, Biochem. J. 364 (2002) 245–254.
[42] U. Wissenbach, G. Schroth, S. Philipp, V. Flockerzi, Structure and mRNA expression of a bovine trp homologue related to mammalian trp2 transcripts, FEBS Lett. 429 (1998) 61–66.
[43] D.D. Billadeau, J.C. Nolz, T.S. Gomez, Regulation of T-cell activation by the cytoskeleton, Nat. Rev. Immunol. 7 (2007) 131–143.
[44] W. Zhang, I. Hirschler-Laszkiewicz, Q. Tong, K. Conrad, S.C. Sun, L. Penn, D.L. Barber, R. Stahl, D.J. Carey, J.Y. Cheung, B.A. Miller, TRPM2 is an ion channel that modulates hematopoietic cell death through activation of caspases and PARP cleavage, Am. J. Physiol. Cell Physiol. 290 (2006) C1146–C1159.
[45] S. Philipp, B. Strauss, D. Hirnet, U. Wissenbach, L. Mery, V. Flockerzi, M. Hoth, TRPC3 mediates T-cell receptor-dependent calcium entry in human T-lymphocytes, J. Biol. Chem. 278 (2003) 26629–26638.
[46] H. Inada, T. Iida, M. Tominaga, Different expression patterns of TRP genes in murine B and T lymphocytes, Biochem. Biophys. Res. Commun. 350 (2006) 762–767.
[47] C. Kunert-Keil, F. Bisping, J. Kruger, H. Brinkmeier, Tissue-specific expression of TRP channel genes in the mouse and its variation in three different mouse strains, BMC Genomics 7 (2006) 159.
[48] E.C. Schwarz, M.J. Wolfs, S. Tonner, A.S. Wenning, A. Quintana, D. Griesemer, M. Hoth, TRP channels in lymphocytes, Handb. Exp. Pharmacol. (2007) 445–456.

[49] G. Spinsanti, R. Zannolli, C. Panti, I. Ceccarelli, L. Marsili, V. Bachiocco, F. Frati, A.M. Aloisi, Quantitative real-time PCR detection of TRPV1-4 gene expression in human leukocytes from healthy and hyposensitive subjects, Mol. Pain 4 (2008) 51.
[50] I.O. Vasil'eva, A. Neguliaev Iu, I.I. Marakhova, S.B. Semenova, [TRPV5 and TRPV6 calcium channels in human T cells], Tsitologiia 50 (2008) 953–957.
[51] U. Wissenbach, B.A. Niemeyer, T. Fixemer, A. Schneidewind, C. Trost, A. Cavalie, K. Reus, E. Meese, H. Bonkhoff, V. Flockerzi, Expression of CaT-like, a novel calcium-selective channel, correlates with the malignancy of prostate cancer, J. Biol. Chem. 276 (2001) 19461–19468.
[52] T. Voets, B. Nilius, TRPs make sense, J. Membr. Biol. 192 (2003) 1–8.
[53] S. Basu, P. Srivastava, Immunological role of neuronal receptor vanilloid receptor 1 expressed on dendritic cells, Proc. Natl Acad. Sci. USA 102 (2005) 5120–5125.
[54] P. Launay, H. Cheng, S. Srivatsan, R. Penner, A. Fleig, J.P. Kinet, TRPM4 regulates calcium oscillations after T cell activation, Science 306 (2004) 1374–1377.
[55] B. Nilius, J. Prenen, G. Droogmans, T. Voets, R. Vennekens, M. Freichel, U. Wissenbach, V. Flockerzi, Voltage dependence of the Ca2+-activated cation channel TRPM4, J. Biol. Chem. 278 (2003) 30813–30820.
[56] X.Z. Xu, F. Moebius, D.L. Gill, C. Montell, Regulation of melastatin, a TRP-related protein, through interaction with a cytoplasmic isoform, Proc. Natl Acad. Sci. USA 98 (2001) 10692–10697.
[57] P. Launay, A. Fleig, A.L. Perraud, A.M. Scharenberg, R. Penner, J.P. Kinet, TRPM4 is a Ca2+-activated nonselective cation channel mediating cell membrane depolarization, Cell 109 (2002) 397–407.
[58] R. Takezawa, H. Cheng, A. Beck, J. Ishikawa, P. Launay, H. Kubota, J.P. Kinet, A. Fleig, T. Yamada, R. Penner, A pyrazole derivative potently inhibits lymphocyte Ca2+ influx and cytokine production by facilitating transient receptor potential melastatin 4 channel activity, Mol. Pharmacol. 69 (2006) 1413–1420.
[59] J. Du, J. Xie, L. Yue, Intracellular calcium activates TRPM2 and its alternative spliced isoforms, Proc. Natl Acad. Sci. USA 106 (2009) 7239–7244.
[60] Y. Hara, M. Wakamori, M. Ishii, E. Maeno, M. Nishida, T. Yoshida, H. Yamada, S. Shimizu, E. Mori, J. Kudoh, N. Shimizu, H. Kurose, Y. Okada, K. Imoto, Y. Mori, LTRPC2 Ca2+-permeable channel activated by changes in redox status confers susceptibility to cell death, Mol. Cell 9 (2002) 163–173.
[61] G.K. Rao, N.E. Kaminski, Induction of intracellular calcium elevation by {Delta}9-tetrahydrocannabinol in T cells involves TRPC1 channels, J. Leukoc. Biol. 79 (2006) 202–213.
[62] M. Schaefer, Homo- and heteromeric assembly of TRP channel subunits, Pflugers Arch. 451 (2005) 35–42.
[63] J.P. Yuan, W. Zeng, G.N. Huang, P.F. Worley, S. Muallem, STIM1 heteromultimerizes TRPC channels to determine their function as store-operated channels, Nat. Cell Biol. 9 (2007) 636–645.
[64] E. Donnadieu, A. Trautmann, Is there a Na+/Ca2+ exchanger in macrophages and in lymphocytes? Pflugers Arch. 424 (1993) 448–455.
[65] Y. Liao, C. Erxleben, E. Yildirim, J. Abramowitz, D.L. Armstrong, L. Birnbaumer, Orai proteins interact with TRPC channels and confer responsiveness to store depletion, Proc. Natl Acad. Sci. USA 104 (2007) 4682–4687.
[66] Y. Liao, C. Erxleben, J. Abramowitz, V. Flockerzi, M.X. Zhu, D.L. Armstrong, L. Birnbaumer, Functional interactions among Orai1, TRPCs, and STIM1 suggest a STIM-regulated heteromeric Orai/TRPC model for SOCE/Icrac channels, Proc. Natl Acad. Sci. USA 105 (2008) 2895–2900.
[67] Y. Liao, N.W. Plummer, M.D. George, J. Abramowitz, M.X. Zhu, L. Birnbaumer, A role for Orai in TRPC-mediated Ca2+ entry suggests that a TRPC:Orai complex may mediate store and receptor operated Ca2+ entry, Proc. Natl Acad. Sci. USA 106 (2009) 3202–3206.